

# Isoform-specific antagonists of exchange proteins directly activated by cAMP

Tamara Tsalkova<sup>a,1</sup>, Fang C. Mei<sup>a,1</sup>, Sheng Li<sup>b</sup>, Oleg G. Chepurny<sup>c</sup>, Colin A. Leech<sup>c</sup>, Tong Liu<sup>b</sup>, George G. Holz<sup>c,d</sup>, Virgil L. Woods, Jr.<sup>b</sup>, and Xiaodong Cheng<sup>a,2</sup>

<sup>a</sup>Department of Pharmacology and Toxicology, Sealy Center for Structural Biology and Molecular Biophysics, University of Texas Medical Branch, Galveston, TX 77555; <sup>b</sup>Department of Medicine and Biomedical Sciences Graduate Program, University of California at San Diego, La Jolla, CA 92093; and Departments of <sup>c</sup>Medicine and <sup>d</sup>Pharmacology, State University of New York, Upstate Medical University, Syracuse, NY 13210

Edited\* by Joseph A. Beavo, University of Washington School of Medicine, Seattle, WA, and approved September 26, 2012 (received for review June 15, 2012)

The major physiological effects of cAMP in mammalian cells are transduced by two ubiquitously expressed intracellular cAMP receptors, protein kinase A (PKA) and exchange protein directly activated by cAMP (EPAC), as well as cyclic nucleotide-gated ion channels in certain tissues. Although a large number of PKA inhibitors are available, there are no reported EPAC-specific antagonists, despite extensive research efforts. Here we report the identification and characterization of noncyclic nucleotide EPAC antagonists that are exclusively specific for the EPAC2 isoform. These EPAC2-specific antagonists, designated as ESI-05 and ESI-07, inhibit Rap1 activation mediated by EPAC2, but not EPAC1, with high potency *in vitro*. Moreover, ESI-05 and ESI-07 are capable of suppressing the cAMP-mediated activation of EPAC2, but not EPAC1 and PKA, as monitored in living cells through the use of EPAC- and PKA-based FRET reporters, or by the use of Rap1-GTP pull-down assays. Deuterium exchange mass spectroscopy analysis further reveals that EPAC2-specific inhibitors exert their isoform selectivity through a unique mechanism by binding to a previously undescribed allosteric site: the interface of the two cAMP binding domains, which is not present in the EPAC1 isoform. Isoform-specific EPAC pharmacological probes are highly desired and will be valuable tools for dissecting the biological functions of EPAC proteins and their roles in various disease states.

cAMP-regulated guanine nucleotide exchange factor | high-throughput screening | hydrogen/deuterium exchange mass spectrometry

Identification of small chemical probes capable of selectively targeting a specific component of the complex cellular signaling network is a major goal of modern pharmacology. The prototypic cAMP second messenger system represents one of the most elaborate and complex signaling networks in biology. It is regulated at multiple levels by multiple families of pharmacologically important signaling molecules, including various G protein coupled receptors, G proteins, adenylate cyclases, and phosphodiesterases. Therefore, it is not surprising that current pharmacological therapeutics target the cAMP signaling pathway more than any other pathways. For many years it was believed that the effects of cAMP in eukaryotes were mediated primarily by the classic cAMP receptor designated as protein kinase A (PKA). However, the discovery of the exchange protein directly activated by cAMP (EPAC) has created a new paradigm for understanding cAMP signaling processes (1, 2). Sharing an evolutionally conserved cAMP binding domain (CBD) with the regulatory subunits of PKA, EPACs are single polypeptide chain proteins with guanine nucleotide exchange activity for small GTPases, Rap1 and Rap2. Among the two known mammalian EPAC isoforms, EPAC1 is ubiquitously expressed in all major tissues, whereas EPAC2 is mainly restricted to the brain, pancreas, and adrenal gland (1, 2). Consistent with this tissue-specific expression pattern of EPAC isoforms, EPAC1 has been implicated in cardiac hypertrophy (3, 4), fibrosis (5-7), and cancers (8-10), as well as leptin resistance (11), whereas EPAC2

is involved in diabetes/insulin secretion (12-18) and autism/depression (19-21).

The existence of two families of ubiquitously expressed and highly coordinated cAMP intracellular receptors provides a mechanism for a more precise and integrated control of the cAMP signaling pathways in a spatial and temporal manner; it also presents a significant challenge for distinguishing the role of EPAC and PKA within the overall cAMP-mediated signaling network (22). Although a number of pharmacological inhibitors of PKA have been valuable for studying its functions (23), currently neither EPAC-specific antagonists nor any chemical probes (agonists or antagonists) that are capable of differentiating EPAC isoforms are available for a selective pharmacological manipulation of the EPAC-mediated signaling pathways. In this study, we describe the identification and characterization of two EPAC-specific antagonists that are exclusively selective for the EPAC2 isoform.

## Results and Discussion

To identify small chemical probes that are capable of specifically inhibiting EPAC, we developed a sensitive and robust high-throughput screening (HTS) assay (24). The assay is based on the fact that a dramatic increase of fluorescence was observed when 8-NBD-cAMP [8-(2-[7-Nitro-4-benzofurazanyl] aminoethyl-thio) adenosine-3', 5'-cyclic monophosphate] was titrated with purified full-length EPAC2, which allows the robust identification of compounds capable of competing with 8-NBD-cAMP binding to EPAC2 under a 384-well format (Fig. S1). Through a screen of a collection of 14,400 druglike, chemically diverse small molecules, we identified seven compounds (Fig. S2) that were able to completely inhibit EPAC2 guanine nucleotide exchange activity to basal levels when these compounds were tested at a 25- $\mu$ M concentration in the presence of an equal concentration of cAMP (Fig. S3A). Because these antagonists were identified using EPAC2 as a target, we tested whether these compounds were also effective in suppressing cAMP-mediated EPAC1 guanine nucleotide exchange factor (GEF) activity. All seven compounds except ESI-05 and ESI-07 were also capable of suppressing EPAC1 GEF activity to basal levels at a 25- $\mu$ M concentration in the presence of an equal concentration of cAMP (Fig. S3B). As shown in Fig. 1A, whereas compounds ESI-05 and ESI-07 inhibited cAMP-mediated EPAC2 GEF activity with apparent  $IC_{50}$  of  $0.43 \pm 0.05$  and  $0.7 \pm 0.1$   $\mu$ M, respectively, they were completely ineffective in suppressing EPAC1 GEF activity. To

Author contributions: T.T., F.C.M., G.G.H., V.L.W., and X.C. designed research; T.T., F.C.M., S.L., O.G.C., C.A.L., and X.C. performed research; T.T., F.C.M., S.L., T.L., G.G.H., V.L.W., and X.C. analyzed data; and X.C. wrote the paper.

The authors declare no conflict of interest.

\*This Direct Submission article had a prearranged editor.

<sup>1</sup>T.T. and F.C.M. contributed equally to this work.

<sup>2</sup>To whom correspondence should be addressed. E-mail: xcheng@utmb.edu.

This article contains supporting information online at [www.pnas.org/lookup/suppl/doi:10.1073/pnas.1210209109/-DCSupplemental](http://www.pnas.org/lookup/suppl/doi:10.1073/pnas.1210209109/-DCSupplemental).

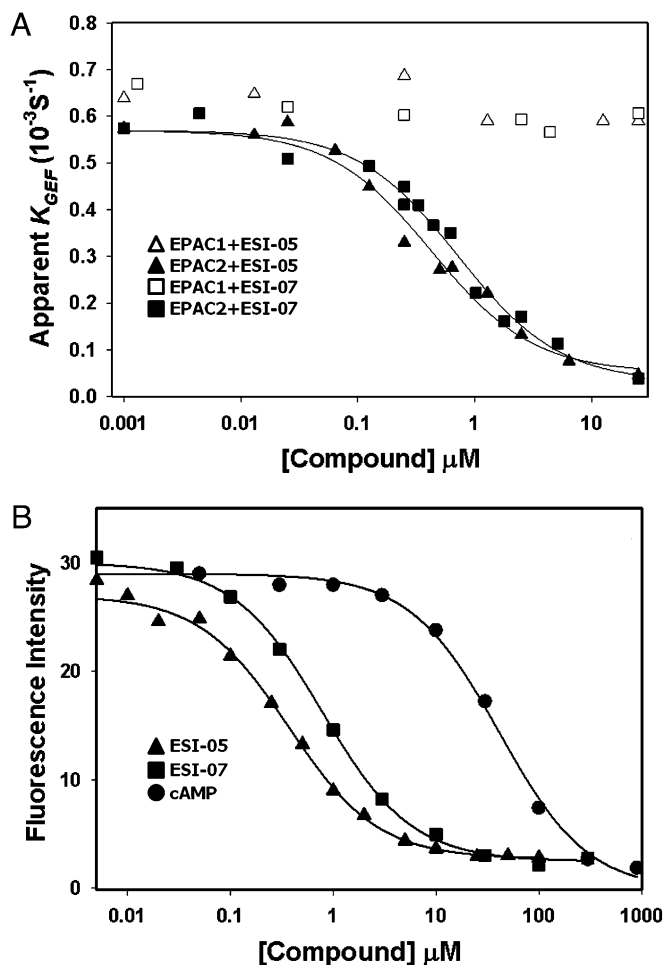


**Fig. 1.** Relative potency of EPAC2 specific antagonists. (A) EPAC GEF activity was monitored as a decrease in fluorescence of a reaction mixture containing 100 nM EPAC, 200 nM Rap-mantGDP, 25  $\mu M$  GDP, and 25  $\mu M$  cAMP. The  $K_{GEF}$  activities at individual ESI concentrations were calculated by fitting the kinetic traces to a single exponential decay. Apparent  $IC_{50}$  values were obtained by plotting individual reaction rates of EPAC1 (open symbols) or EPAC2 (filled symbols) against the ESI-05 (triangles) and ESI-07 (squares) concentrations. (B) Dose-dependent competition of ESI-05 (triangles), ESI-07 (squares), and cAMP (circles) with 8-NBD-cAMP in binding to EPAC2. Similar results were obtained from three independent titrations. Apparent  $IC_{50}$  values were obtained by fitting of the individual titration curves and expressed in the format of means and SDs.

determine the relative binding affinity of ESI-05 and ESI-07 to EPAC2, we performed dose-dependent titrations to test the ability of these compounds to compete with the binding of 8-NBD-cAMP to EPAC2. When various concentrations of cAMP or EPAC2 antagonists were added to reaction mixture with fixed concentrations of EPAC2 and 8-NBD-cAMP, a dose-dependent decrease in 8-NBD-cAMP fluorescence was observed (Fig. 1B). Whereas cAMP competed with 8-NBD-cAMP binding with an apparent  $IC_{50}$  of  $40 \pm 1 \mu M$ , ESI-05 and ESI-07 showed an increased potency with apparent  $IC_{50}$  of  $0.4 \pm 0.1$  and  $0.6 \pm 0.1 \mu M$ , respectively, representing a 100- or 67-fold increase in affinity over cAMP. To further test the specificity of ESI-05 and ESI-07, we performed counter-screening assays that measure type I and II PKA holoenzyme activities, respectively. ESI-05 and ESI-07 (25  $\mu M$ ) did not significantly alter type I and II PKA holoenzyme activation in the presence and absence of 100- $\mu M$  cAMP, whereas H89, a selective PKA inhibitor, blocked the type I and II PKA activities completely (Fig. S4).

To test whether our identified EPAC2 antagonists were capable of selectively modulating EPAC activation in living cells, we monitored the ability of ESI-05 and ESI-07 to suppress EPAC-mediated Rap1 cellular activation using HEK293 cells stably expressing EPAC1 or EPAC2 (Fig. S5). As shown in Fig. 2A, when HEK293 cells that ectopically express full-length EPAC2 proteins were treated with the EPAC-selective cAMP analog 8-(4-Chlorophenylthio)-2'-O-methyladenosine-3',5'-cyclic monophosphate acetoxymethyl ester (007-AM), an increase in the fraction of GTP-bound cellular Rap1 was observed. Pretreatment of HEK293/EPAC2 cells with 1, 5, 10, and 25  $\mu M$  ESI-05 led to a dose-dependent reduction of 007-AM induced Rap1 activation, whereas ESI-05 alone at 25  $\mu M$  had no effect on Rap1 activation. Similar results were obtained using ESI-07 (Fig. 2B). However, when HEK293 cells ectopically expressing full-length EPAC1 proteins were used, compounds ESI-05 and ESI-07 were completely ineffective at a 25- $\mu M$  concentration (Fig. 2C). These results are consistent with the biochemical Rap1 exchange data shown in Fig. 1A and confirm that compounds ESI-05 and ESI-07 are EPAC2-specific antagonists.

To confirm that ESI-05 and ESI-07 are EPAC2 isoform-specific antagonists, we further tested the compounds using HEK293 cells stably expressing an EPAC2- or EPAC1-based fluorescence resonance energy transfer (FRET) sensor (25), EPAC2-FL, EPAC1-FL, or EPAC1-camps (26). As expected, stimulation of HEK293/EPAC2-FL cells by 3  $\mu M$  007-AM led to an increase of FRET measured as an increase of the 485/535 nm emission ratio using a FlexStation 3 microplate reader (Fig. 3A and Fig. S6). Pretreatment of HEK293/EPAC2-FL cells with 10  $\mu M$  ESI-05 fully blocked the 007-AM-induced decrease of FRET (Fig. 3B and C), as well as the decrease of FRET induced by the cAMP-elevating agents forskolin and isobutylmethylxanthine under conditions of live-cell imaging using HEK293/EPAC2-FL cells (Fig. S7). In contrast, when experiments were performed using HEK293 cells stably expressing an EPAC1 FRET reporter (HEK293/EPAC1-FL cells), we found that ESI-05 failed to block the action of 007-AM to decrease FRET (Fig. 3D–F). Moreover, ESI-05 was also unable to block EPAC1-camps activation in response to forskolin and isobutylmethylxanthine (Fig. 3G and H). In addition, using HEK293 cells stably expressing the PKA sensor AKAR3 (27), it was also possible to demonstrate that the stimulatory action of 8-Br-cAMP at PKA was not inhibited by ESI-05 (Fig. S8). Subsequent experiments then revealed that these findings obtained with ESI-05 were reproducible using ESI-07; ESI-07 failed to block AKAR3 activation (Fig. S8), whereas it exerted a dose-dependent effect to block the activation of EPAC2-FL, but not EPAC1-camps (Fig. S9).

Because ESI-05 and ESI-07 were identified using EPAC2 as a direct target, it is not surprising that they are more selective inhibitors toward EPAC2 than toward EPAC1. However, it was quite unexpected that they are exclusively specific for EPAC2 without apparent activity toward EPAC1. The existence of selective inhibitors capable of differentiating between EPAC1 and EPAC2 suggests that although EPAC1 and 2 share extensive sequence homology there are also significant structural differences that can be explored pharmacologically using small chemical compounds. To investigate the potential mechanism of action of these EPAC-specific inhibitors, we examined the effect of ESI-07 binding on EPAC2 protein structure by monitoring the rates of amide hydrogen exchange using deuterium exchange mass spectrometry (DXMS). This technique has proven valuable for studying the mechanism of activation of EPAC by providing structural information regarding the mode of cAMP binding and conformational changes associated with EPAC activation (28, 29). Incubation of ESI-07 with full-length EPAC2 proteins led to significant reductions of H/D exchange rates in several regions of EPAC2, including peptide fragments 104–118, 119–129, and 386–417 (Fig. 4 and Fig. S10). As shown in Fig. 5, when the regions with decreased solvent accessibility in response to ESI-07

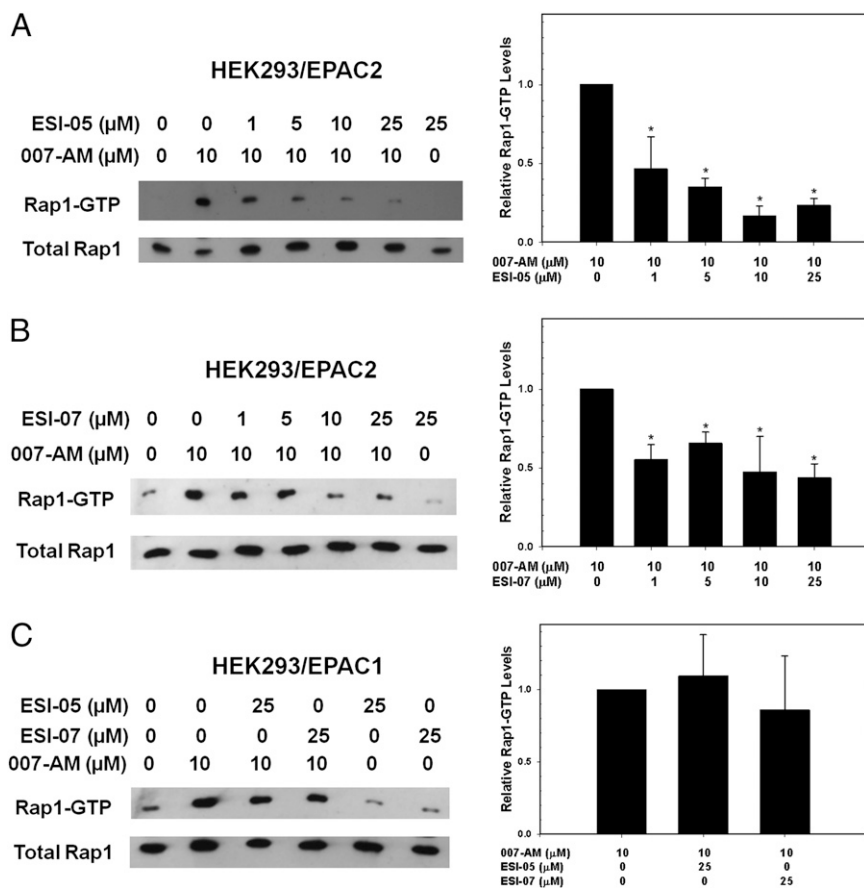


**Fig. 2.** Effects of EPAC2-specific antagonists on 007-AM-mediated cellular activation of Rap1. Serum-starved HEK293/EPAC2 cells or HEK293/EPAC1 cells with or without pretreatment of ESI-05 or ESI-07 for 5 min were stimulated with 10  $\mu\text{M}$  007-AM for 10 min. GTP-bound Rap1 (Rap1GTP) obtained by a Ral-GDS-RBD-GST pull-down assay and total cellular Rap1 were detected by immunoblotting with Rap1-specific antibody. (A) HEK293/EPAC2 cells treated with ESI-05. (B) HEK293/EPAC2 cells treated with ESI-07. (C) HEK293/EPAC1 cells treated with ESI-05 or ESI-07. Similar results were obtained with three independent experiments for each panel of Fig. 2. A *t* test was used to determine statistical significance ( $*P < 0.05$ ).

binding were mapped onto the crystal structure of apo-EPAC2, they defined a continuous area in three dimensions spanning the interface between the two CBDs that are arranged in a face-to-face configuration to form a continuous structural lobe in the apo-EPAC2 crystal structure (29–31). However, cAMP binding to EPAC2 protected additional flanking areas on both CBDs (29). In addition, unlike cAMP, binding of ESI-07 to EPAC2 did not lead to an increase in H/D exchange in a critical region, the hinge/switchboard, which undergoes a dramatic conformational change in response to cAMP binding during EPAC activation: the hinge helix swings closer to the core of the CBD-B and the last two turns of the hinge helix dissolve into an extended loop. To the contrary, a decrease in H/D exchange was observed for the corresponding hinge peptide (436–446) in response to ESI-07 binding. Taken together, these data are consistent with a model that ESI-07 functions by binding to the interfaces of two CBDs on EPAC2 and locks the protein in its autoinhibitory conformation. This finding is consistent with the fact that ESI-07 is exclusively specific for EPAC2; EPAC1 contains only one CBD and therefore is not compatible for ESI-07 binding. Our results do not exclude the possibility that ESI-07 binds to another unidentified allosteric site on EPAC2 and prevents the activation of EPAC2 by stabilizing the inactive conformation. However, this scenario is unlikely, because we did not observe significant ESI-07-induced solvent protection outside the CBD interface.

In summary, we describe the identification and characterization of a number of noncyclic nucleotide small compounds that effectively inhibit EPAC functions both at the biochemical and cellular levels using purified protein components or intact cells. Moreover, we provide a structural explanation why ESI-05 and ESI-07 act as exclusive EPAC2-specific inhibitors. These isoform-specific EPAC inhibitors will be valuable tools for dissecting the isoform-specific functions of EPAC proteins.

### Experimental Procedures

**Reagents.** The 007-AM and 8-NBD-cAMP were purchased from BioLog Life Science Institute. MANT-GDP was from Invitrogen. All other reagents were purchased through Sigma-Aldrich.

**Protein Expression and Purification.** Recombinant EPAC1, EPAC2, and C-terminal truncated Rap1B(1–167) were purified as described previously (32). PKA R $\alpha$ , RII $\beta$ , and catalytic subunits were recombinantly expressed in *Escherichia coli* and purified to homogeneity as reported (33). Type I and II PKA holoenzymes were reconstituted from individually purified recombinant PKA R and C subunits (34). All proteins used in this study were at least 95% pure, as judged by SDS PAGE.

**Primary HTS Assay.** Primary screening of the Maybridge HitFinder library (Thermo Fisher Scientific) was performed in black, 384-well, low-volume microplates using a high-throughput screening assay described previously (24).

**Secondary Assay.** A well-established biochemical GEF activity assay of EPAC proteins was used a secondary assay to confirm the initial hits from the primary HTS screens. In vitro EPAC activity was measured using purified

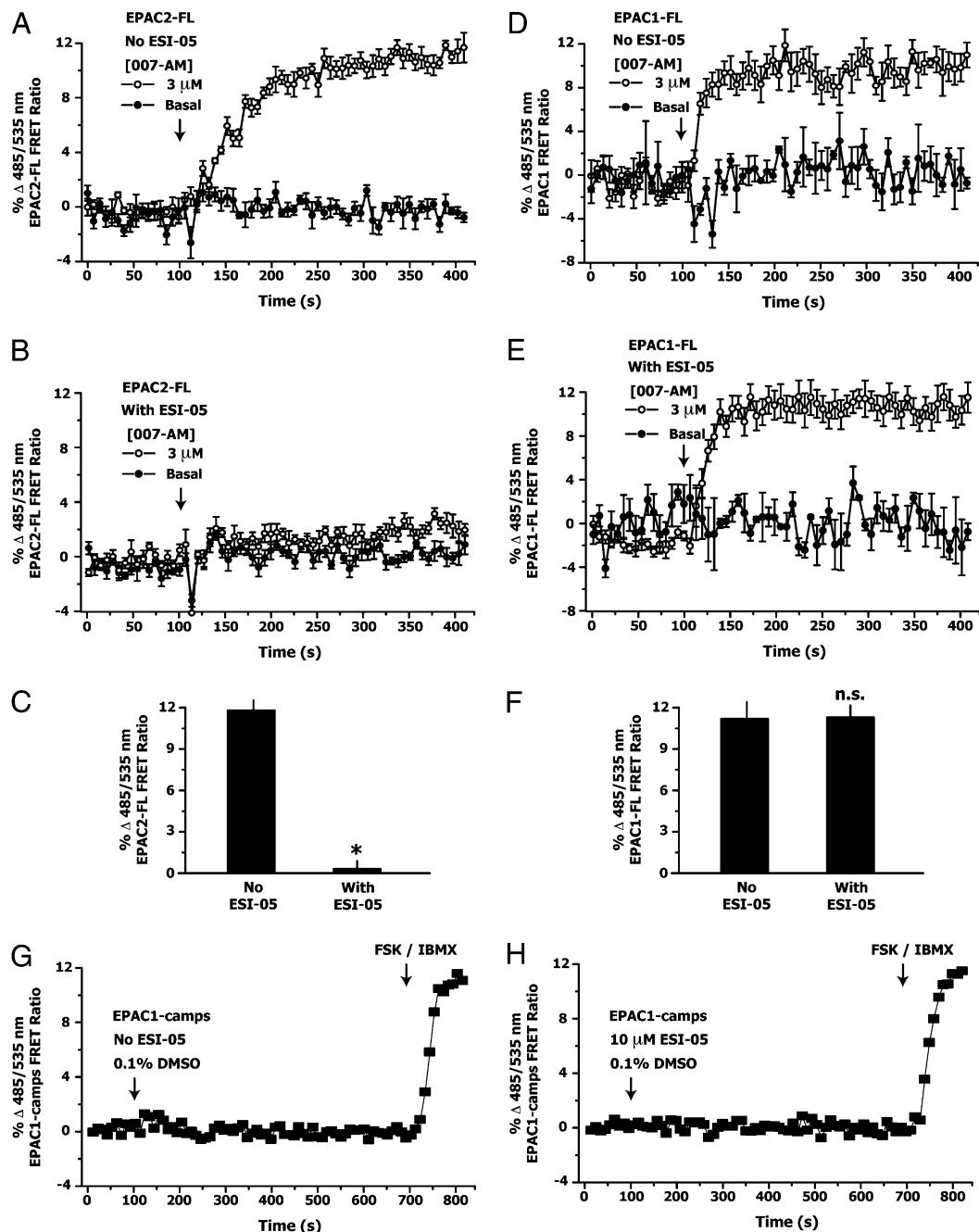


**Fig. 3.** Suppressing of cellular activation of EPAC2-FL but not EPAC1-FL or EPAC1-camps by ESI-05. For HEK293 cells stably expressing EPAC2-FL (A–C), EPAC1-FL (D–F), or EPAC1-camps (G, H), it was demonstrated that 10  $\mu$ M ESI-05 blocked EPAC2-FL but not EPAC1-FL or EPAC1-camps activation in response to 3  $\mu$ M 007-AM or 2  $\mu$ M forskolin and 100  $\mu$ M isobutylmethylxanthine, respectively. Similar results were obtained with three independent experiments for each panel of Fig. 3. A *t* test was used to determine statistical significance (\**P* < 0.05).

recombinant full-length EPAC proteins and Rap1B (1–167) loaded with Mant-GDP as described previously (35).

**Counter-Screening Assay.** In vitro PKA kinase activities of the type I and II PKA holoenzymes were measured spectrophotometrically with a coupled enzyme assay using a synthetic peptide, Kempetide, as a substrate in a 96-well plate as described previously (36).

**Cellular Rap1 Activation Assay.** HEK 293 cells that stably expresses full-length human EPAC1 or mouse EPAC2 were established as described previously and were grown in DMEM with 10% (vol/vol) FBS (37). The cultures were maintained at 37 °C in a humidified chamber supplemented with 5% CO<sub>2</sub>. Cellular activation of Rap1 was determined by pull-down of lysates derived

from HEK293 cells stably expressing individual EPAC isoform using Ral-GDS-RBD-GST affinity beads as described earlier (32).

**Deuterium Exchange Mass Spectrometry.** The optimal quench conditions that generate the best pepsin cleavage peptide coverage maps of EPAC2 were obtained as previously described (29). Functionally deuterated protein samples were prepared at 0 °C by mixing 2.5  $\mu$ L of stock solution of EPAC2 (3.5 mg/mL), in the presence or absence of 300  $\mu$ M ESI-07, with 7.5  $\mu$ L of deuterated buffer (8.3 mM Tris, 150 mM NaCl, 1 mM DTT, and 1 mM EDTA in D<sub>2</sub>O) and incubating for 10, 100, 1,000, 10,000, or 100,000 seconds. At the indicated time, the exchange reaction was quenched by addition of 15  $\mu$ L of ice-cold optimal quench solution (0.8% formic acid, 16.6% glycerol, and 1.6 M GuHCl) and then immediately frozen on dry ice and stored at

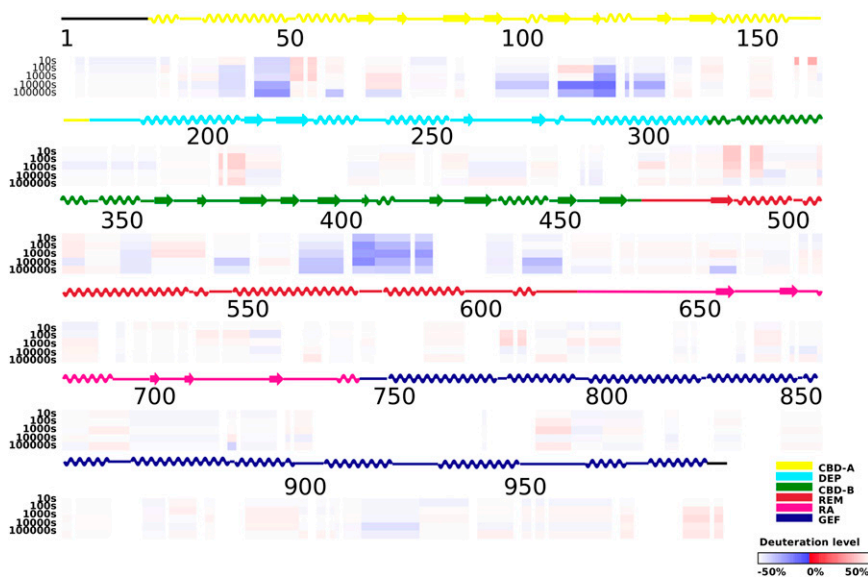


**Fig. 4.** Changes in hydrogen/deuterium exchange rates of EPAC2 induced by binding of ESI-07. Differences in deuteration levels in the free and ESI-07-bound EPAC2 at various time points (from top to bottom: 10, 100, 1,000, 10,000, and 100,000 s) are shown in color-coded bars ranging from blue (−50%) to red (50%), as indicated at the bottom right corner of the figure.

−80 °C. Nondeuterated control samples were prepared in H<sub>2</sub>O buffer (8.3 mM Tris, 150 mM NaCl, 1 mM DTT, and 1 mM EDTA in H<sub>2</sub>O) and equilibrium-deuterated samples (incubated in D<sub>2</sub>O buffer containing 0.5% formic acid

for 1 d at 25 °C) were also prepared. The samples were then thawed at 5 °C and immediately passed over tandem protease columns (porcine pepsin, 16- $\mu$ L bed volume, followed by *Aspergillus saitoi* fungal protease type XIII, 16  $\mu$ L bed volume) with 0.05% TFA in water at a flow rate of 20  $\mu$ L/min for 6 min. The proteolytic fragments were collected contemporaneously on a C18 guard column (Magic C18AQ, 0.2  $\times$  2; Michrom), desalted for 1 min at 60  $\mu$ L/min, and separated on a Michrom reversed-phase C18 column (Magic C18AQ, 3  $\mu$ , 200A, 0.2  $\times$  50) with a linear gradient of acetonitrile from 6.4% to 38.4% (vol/vol) over 30 min. The eluant was directed to a Finnigan LCQ Classic mass spectrometer with electrospray ionization voltage set at 4.5 kV, capillary temperature at 200 °C, and data acquisition in either MS1 profile mode or data-dependent MS/MS mode. The SEQUEST software (Thermo Finnigan) was used for peptide identification, and specialized software, DXMS Explorer (Sierra Analytics Inc.), was used to determine deuteration level of peptides in functionally deuterated samples as previously described (38, 39).

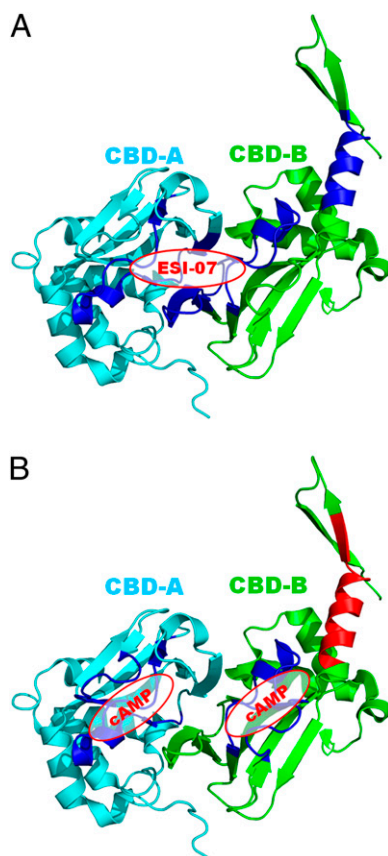


**Fig. 5.** Mechanism of ESI-07-mediated isoform-specific EPAC2 antagonism. (A) Proposed model of ESI-07 binding to EPAC2. Areas within CBD-A (cyan) and CBD-B (green) of EPAC2 (2BYV) with reduced H/D exchange rates in response to ESI-07 binding are shown in dark blue. (B) Proposed model of cAMP binding to EPAC2. Areas within CBD-A (cyan) and CBD-B (green) of EPAC2 (2BYV) with reduced H/D exchange rates in response to cAMP binding are shown in dark blue; the area with increased H/D exchange rates in response to cAMP binding is shown in red (29).

**FRET-Based Assay for EPAC1-FL, EPAC2-FL, EPAC1-camps, or AKAR3 Activation.** HEK cells were stably transfected with genetically encoded biosensors in which the full-length EPAC1 or EPAC2 proteins were fused at their N termini to a Cerulean variant of CFP and at their C termini to a Venus variant of YFP (25). HEK cells were also stably transfected with the EPAC1-camps reporter in which the cyclic nucleotide-binding domain of EPAC1 was fused at its N terminus to a variant of YFP and at its C terminus to a variant of CFP (26). Activation of EPAC1-FL, EPAC2-FL, or EPAC1-camps in response to cAMP was measured as a decrease of FRET, and it was plotted as an increase of the CFP/YFP emission ratio (i.e., 485/535 nm emission ratio). AKAR3 incorporates a variant of CFP at its N terminus and a variant of YFP at its C terminus. A phosphoamino acid-binding domain and a PKA substrate motif within AKAR3 together act as a linker (27). Activation of AKAR3 in response to cAMP was measured as an increase of FRET, and it was plotted as a decrease of the 485/535 nm emission ratio. The individual HEK cell clones reported here are EPAC1-C9, EPAC2-C1, EPAC1-camps-C10, and AKAR3-C12. Single-cell suspensions of these clones were plated onto 96-well, clear-bottomed assay plates (3904; Costar) in which individual wells were coated with rat tail collagen (Invitrogen). The clones were maintained in DMEM [25 mM glucose, 10% (vol/vol) FBS] for 24 h to allow the cell cultures to become 80–90% confluent. Spectroscopy was performed as described previously (40) using a FlexStation 3 microplate reader controlled using SoftMax Pro software (Molecular Devices). The time course of the change of FRET ratio was plotted after exporting data to Origin v.7.5 (OriginLab). The excitation light was delivered at 435/9 nm (455 nm cutoff), and the emitted light was detected at 485/15 nm (CFP) or 535/15 nm (YFP). For live-cell imaging of FRET in single cells of the HEK cell clones reported here, the methods of analyses were identical to those reported by Chepurny et al. in prior reports (40, 41).

**ACKNOWLEDGMENTS.** We thank Dr. Jin Zhang of The Johns Hopkins University School of Medicine for providing the EPAC1, EPAC2, and AKAR3 FRET reporters and Drs. Martin J. Lohse and Viacheslav O. Nikolaev for providing the EPAC1-camps reporter. This work is supported by Grant 5R01GM066170 from the National Institutes of Health.

- de Rooij J, et al. (1998) Epac is a Rap1 guanine-nucleotide-exchange factor directly activated by cyclic AMP. *Nature* 396(6710):474–477.
- Kawasaki H, et al. (1998) A family of cAMP-binding proteins that directly activate Rap1. *Science* 282(5397):2275–2279.
- Morel E, et al. (2005) cAMP-binding protein Epac induces cardiomyocyte hypertrophy. *Circ Res* 97(12):1296–1304.
- Métrich M, et al. (2008) Epac mediates beta-adrenergic receptor-induced cardiomyocyte hypertrophy. *Circ Res* 102(8):959–965.
- Yokoyama U, et al. (2008) The cyclic AMP effector Epac integrates pro- and anti-fibrotic signals. *Proc Natl Acad Sci USA* 105(17):6386–6391.
- Villarreal F, Epperson SA, Ramirez-Sanchez I, Yamazaki KG, Brunton LL (2009) Regulation of cardiac fibroblast collagen synthesis by adenosine: roles for Epac and PI3K. *Am J Physiol Cell Physiol* 296(5):C1178–C1184.
- Insel PA, et al. (2012) cAMP and Epac in the regulation of tissue fibrosis. *Br J Pharmacol* 166(2):447–456.
- Lorenz R, Aleksic T, Wagner M, Adler G, Weber CK (2008) The cAMP/Epac1/Rap1 pathway in pancreatic carcinoma. *Pancreas* 37(1):102–103.
- Misra UK, Pizzo SV (2009) Epac1-induced cellular proliferation in prostate cancer cells is mediated by B-Raf/ERK and mTOR signaling cascades. *J Cell Biochem* 108(4):998–1011.
- Baljinnyam E, et al. (2011) Epac1 promotes melanoma metastasis via modification of heparan sulfate. *Pigment Cell Melanoma Res* 24(4):680–687.
- Fukuda M, Williams KW, Gautron L, Elmquist JK (2011) Induction of leptin resistance by activation of cAMP-Epac signaling. *Cell Metab* 13(3):331–339.
- Kashima Y, et al. (2001) Critical role of cAMP-GEFII—Rim2 complex in incretin-potentiated insulin secretion. *J Biol Chem* 276(49):46046–46053.
- Kang G, Chepurny OG, Holz GG (2001) cAMP-regulated guanine nucleotide exchange factor II (Epac2) mediates Ca<sup>2+</sup>-induced Ca<sup>2+</sup> release in INS-1 pancreatic beta-cells. *J Physiol* 536(Pt 2):375–385.
- Kang G, et al. (2003) Epac-selective cAMP analog 8-pCPT-2'-O-Me-cAMP as a stimulus for Ca<sup>2+</sup>-induced Ca<sup>2+</sup> release and exocytosis in pancreatic beta-cells. *J Biol Chem* 278(10):8279–8285.
- Shibasaki T, et al. (2007) Essential role of Epac2/Rap1 signaling in regulation of insulin granule dynamics by cAMP. *Proc Natl Acad Sci USA* 104(49):19333–19338.
- Holz GG (2004) Epac: A new cAMP-binding protein in support of glucagon-like peptide-1 receptor-mediated signal transduction in the pancreatic beta-cell. *Diabetes* 53(1):5–13.
- Zhang CL, et al. (2009) The cAMP sensor Epac2 is a direct target of antidiabetic sulfonylurea drugs. *Science* 325(5940):607–610.
- Mukai E, et al. (2011) Exendin-4 suppresses SRC activation and reactive oxygen species production in diabetic Goto-Kakizaki rat islets in an Epac-dependent manner. *Diabetes* 60(1):218–226.
- Woolfrey KM, et al. (2009) Epac2 induces synapse remodeling and depression and its disease-associated forms alter spines. *Nat Neurosci* 12(10):1275–1284.
- Penzes P, Woolfrey KM, Srivastava DP (2011) Epac2-mediated dendritic spine remodeling: Implications for disease. *Mol Cell Neurosci* 46(2):368–380.
- Yang Y, et al. (2012) EPAC null mutation impairs learning and social interactions via aberrant regulation of miR-124 and Zif268 translation. *Neuron* 73(4):774–788.
- Cheng X, Ji Z, Tsalkova T, Mei F (2008) Epac and PKA: A tale of two intracellular cAMP receptors. *Acta Biochim Biophys Sin (Shanghai)* 40(7):651–662.
- Murray AJ (2008) Pharmacological PKA inhibition: All may not be what it seems. *Sci Signal* 1(22):re4.
- Tsalkova T, Mei FC, Cheng X (2012) A fluorescence-based high-throughput assay for the discovery of exchange protein directly activated by cyclic AMP (EPAC) antagonists. *PLoS ONE* 7(1):e30441.
- Herbst KJ, Coltharp C, Amzel LM, Zhang J (2011) Direct activation of Epac by sulfonylurea is isoform selective. *Chem Biol* 18(2):243–251.
- Nikolaev VO, Bünemann M, Hein L, Hannawacker A, Lohse MJ (2004) Novel single chain cAMP sensors for receptor-induced signal propagation. *J Biol Chem* 279(36):37215–37218.
- Allen MD, Zhang J (2006) Subcellular dynamics of protein kinase A activity visualized by FRET-based reporters. *Biochem Biophys Res Commun* 348(2):716–721.
- Brock M, et al. (2007) Conformational analysis of Epac activation using amide hydrogen/deuterium exchange mass spectrometry. *J Biol Chem* 282(44):32256–32263.
- Li S, et al. (2011) Mechanism of intracellular cAMP sensor Epac2 activation: cAMP-induced conformational changes identified by amide hydrogen/deuterium exchange mass spectrometry (DXMS). *J Biol Chem* 286(20):17889–17897.
- Rehmann H, Das J, Knipscheer P, Wittinghofer A, Bos JL (2006) Structure of the cyclic-AMP-responsive exchange factor Epac2 in its auto-inhibited state. *Nature* 439(7076):625–628.
- Rehmann H, et al. (2008) Structure of Epac2 in complex with a cyclic AMP analogue and RAP1B. *Nature* 455(7209):124–127.
- Mei FC, Cheng XD (2005) Interplay between exchange protein directly activated by cAMP (Epac) and microtubule cytoskeleton. *Mol Biosyst* 1(4):325–331.
- Cheng X, Phelps C, Taylor SS (2001) Differential binding of cAMP-dependent protein kinase regulatory subunit isoforms alpha and Ibeta to the catalytic subunit. *J Biol Chem* 276(6):4102–4108.
- Yu S, Mei FC, Lee JC, Cheng X (2004) Probing cAMP-dependent protein kinase holoenzyme complexes I alpha and II beta by FT-IR and chemical protein footprinting. *Biochemistry* 43(7):1908–1920.
- Tsalkova T, Blumenthal DK, Mei FC, White MA, Cheng X (2009) Mechanism of Epac activation: Structural and functional analyses of Epac2 hinge mutants with constitutive and reduced activities. *J Biol Chem* 284(35):23644–23651.
- Cook PF, Neville ME, Jr., Vrana KE, Hartl FT, Roskoski R, Jr. (1982) Adenosine cyclic 3',5'-monophosphate dependent protein kinase: Kinetic mechanism for the bovine skeletal muscle catalytic subunit. *Biochemistry* 21(23):5794–5799.
- Qiao J, Mei FC, Popov VL, Vergara LA, Cheng X (2002) Cell cycle-dependent subcellular localization of exchange factor directly activated by cAMP. *J Biol Chem* 277(29):26581–26586.
- Pantazatos D, et al. (2004) Rapid refinement of crystallographic protein construct definition employing enhanced hydrogen/deuterium exchange MS. *Proc Natl Acad Sci USA* 101(3):751–756.
- Hamuro Y, et al. (2004) Mapping intersubunit interactions of the regulatory subunit (RIalpha) in the type I holoenzyme of protein kinase A by amide hydrogen/deuterium exchange mass spectrometry (DXMS). *J Mol Biol* 340(5):1185–1196.
- Chepurny OG, et al. (2009) Enhanced Rap1 activation and insulin secretagogue properties of an acetoxymethyl ester of an Epac-selective cyclic AMP analog in rat INS-1 cells: Studies with 8-pCPT-2'-O-Me-cAMP-AM. *J Biol Chem* 284(16):10728–10736.
- Chepurny OG, et al. (2010) PKA-dependent potentiation of glucose-stimulated insulin secretion by Epac activator 8-pCPT-2'-O-Me-cAMP-AM in human islets of Langerhans. *Am J Physiol Endocrinol Metab* 298(3):E622–E633.

# Supporting Information

Tsalkova et al. 10.1073/pnas.1210209109

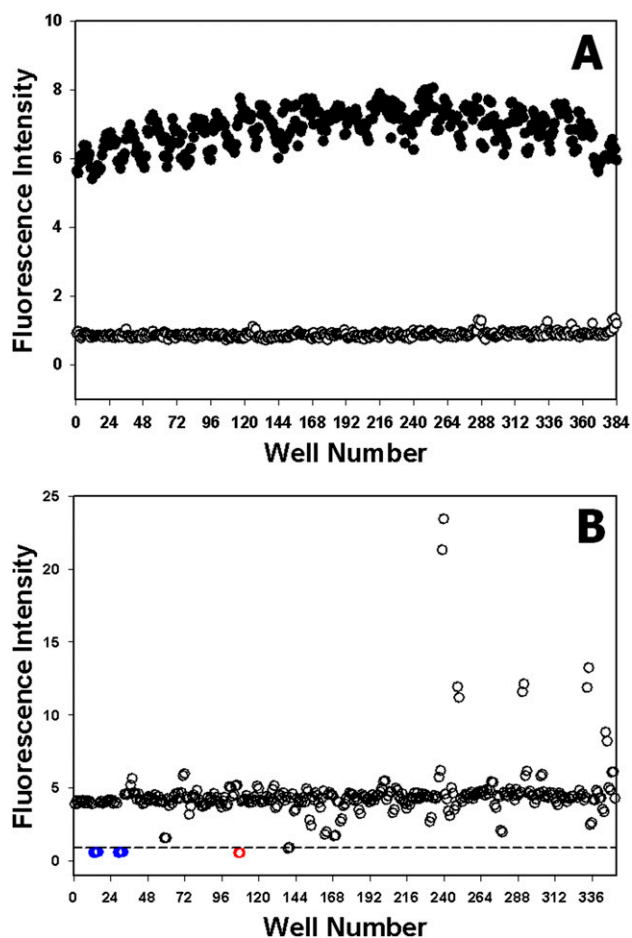


**Fig. S1.** Primary HTS results. (A) Typical control assay data from a test run in 384-well format: fluorescence signals of a solution containing 0.05  $\mu\text{mol}$  of EPAC2 and 0.06  $\mu\text{mol}$  of 8-NBD-cAMP in the absence (filled circles) or presence (open circles) of 300  $\mu\text{M}$  cAMP. The calculated  $Z'$  value is 0.7. (B) Typical screen data: fluorescence signals of a solution containing 0.05  $\mu\text{mol}$  of EPAC2 and 0.06  $\mu\text{mol}$  of 8-NBD-cAMP in the presence of 278  $\mu\text{mol}$  of the individual test compounds (black circles, duplicates) or 300  $\mu\text{mol}$  of cAMP (blue circles, positive control). The dashed line represents the cutoff threshold for positive hits. Red circles indicate an initial hit (ESI-05). Compounds with auto-fluorescence under the assay conditions show increased fluorescence signals.



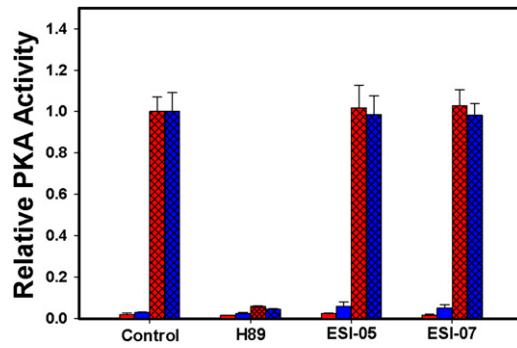


**Fig. 54.** Effects of ESI-05 and ESI-07 on type I and II PKA activities. Relative type I (red) and II (blue) PKA holoenzyme activities in the absence (solid bars) or presence (cross-hatched bars) of 100  $\mu$ M cAMP plus vehicle control, 25  $\mu$ M H-89, 25  $\mu$ M ESI-05, or 25  $\mu$ M ESI-07. Data are presented in the format of means and SDs ( $n = 3$ ).

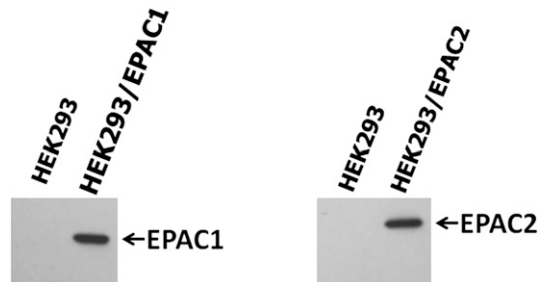


**Fig. 55.** Expression levels of EPAC1 and EPAC2 in HEK293 cells with or without ectopic expression of EPAC1 or EPAC2. Relative cellular levels of EPAC1 and EPAC2 as probed by EPAC1 or EPAC2 specific antibodies, respectively.



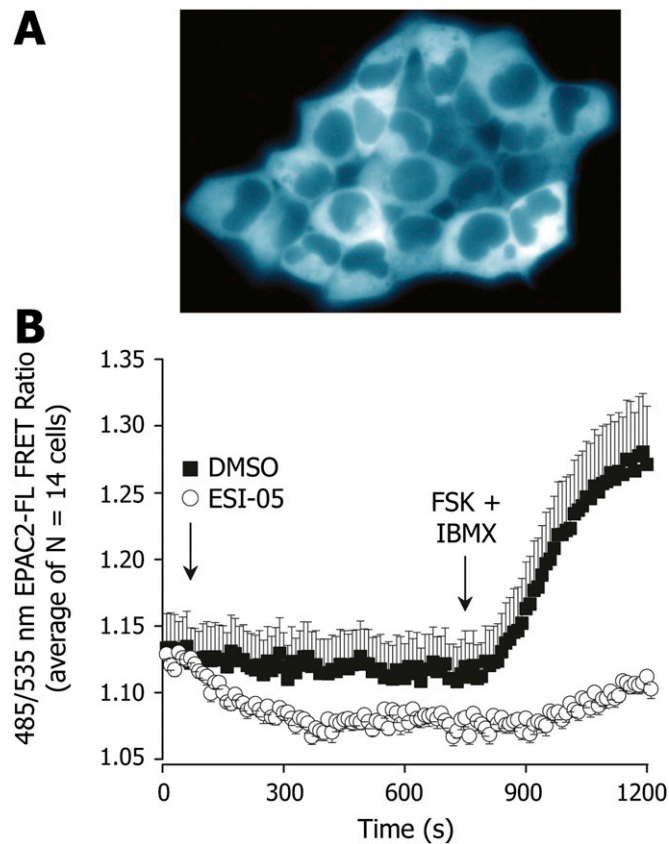


**Fig. S7.** Imaging of EPAC2-FL activation. (A) HEK293 cells stably expressing the EPAC2-FL FRET reporter, as imaged using a 63 $\times$  Nikon TIRF objective, a Nikon Ti inverted microscope, and a Photometrics Cascade II EMCCD camera under the control of Metafluor software. (B) The 485/535 nm FRET ratios determined by imaging these same cells under conditions of superfusion. For the data shown by filled squares, the experiment was started using a superfusate composed of standard extracellular saline (SES). At the time point indicated by the left arrow, the superfusate was switched to SES containing 0.1% DMSO. Subsequently, at the time point indicated by the right arrow, the superfusate was switched to SES containing 0.1% DMSO and 2  $\mu$ M forskolin (FSK) and 100  $\mu$ M isobutylmethylxanthine (IBMX). For data shown by open circles, the experiment was started using a superfusate composed of SES, and at the time point indicated by the left arrow the superfusate was switched to SES containing 10  $\mu$ M ESI-05. Note that ESI-05 produced a decrease of 485/535 nm FRET ratio, as expected if ESI-05 inhibited basal EPAC2-FL activity. Also note that in the presence of ESI-05 the action of FSK/IBMX was blocked (right arrow). Individual data points are the averages of  $n = 14$  HEK293 cells stably expressing the EPAC2-FL FRET reporter. All measurements were obtained at room temperature.



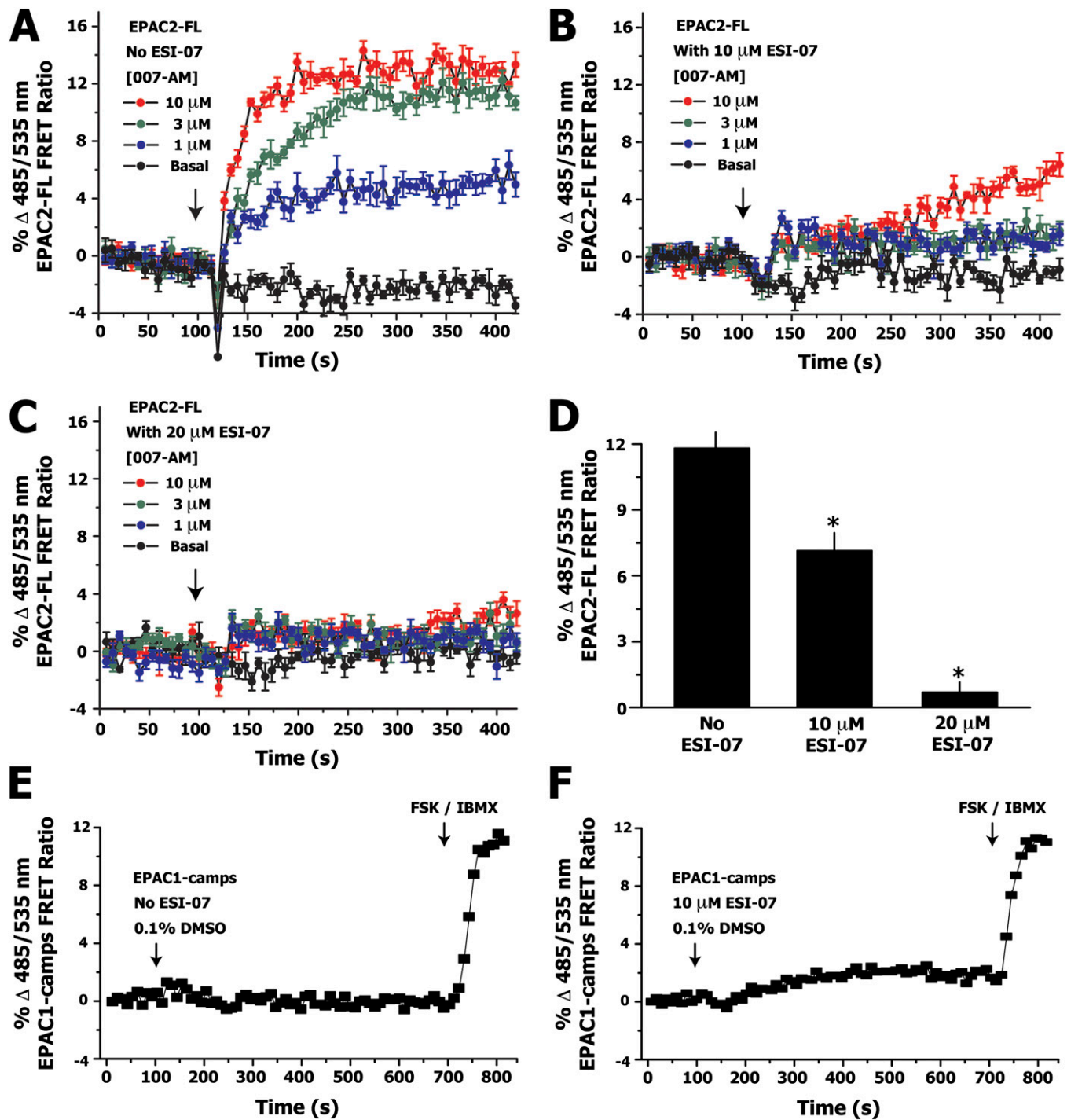


**Fig. 59.** ESI-07 prevents EPAC2-FL activation but not EPAC1-camps activation. For control conditions (A) it was possible to measure the effect of 007-AM (application indicated by the arrow) to activate the EPAC2-FL FRET reporter stably expressed in HEK293 cells grown as monolayers on a 96-well plate. This action of 007-AM measured using a FlexStation 3 was antagonized under conditions in which HEK293 cells were pretreated with ESI-07 at a concentration of 10  $\mu\text{M}$  (B) or 20  $\mu\text{M}$  (C). By determining the maximal change of FRET ratio measured at the 400-s time interval, it was possible to quantify the antagonistic action of 10 or 20  $\mu\text{M}$  ESI-07 versus 10  $\mu\text{M}$  007-AM. (D) A *t* test was used to determine statistical significance ( $*P < 0.05$ ). Complementary assays using the EPAC1-camps reporter demonstrated that the effects of forskolin (FSK, 2  $\mu\text{M}$ ) and isobutylmethylxanthine (IBMX, 100  $\mu\text{M}$ ) to activate this reporter (E) were not blocked by pretreatment of stably transfected HEK293/EPAC1-camps cells with 10  $\mu\text{M}$  ESI-07 (F).

